A POPULATION-BASED PHARMACOKINETIC MODEL APPROACH TO PANTOPRAZOLE DOSING FOR OBESE CHILDREN AND ADOLESCENTS

Valentina Shakhnovich, MD[a], **P Brian Smith, MD, MHS, MPH**[b], **Jeffrey T Guptill, MD, MA, MHS**[b], **Laura P James, MD**[c], **David N Collier, MD, PhD, FAAP**[d], **Huali Wu, PhD**[b], **Chad E Livingston, MBA**[b], **Jian Zhao, PhD**[e], **Gregory L Kearns, PharmD, PhD**[c], and **Michael Cohen-Wolkowiez, MD**[b] **the Best Pharmaceuticals for Children Act – Pediatric Trials Network**[f]

[a]The Children's Mercy Hospital, Kansas City, MO;

[b]Duke Clinical Research Institute, Durham, NC;

[c]Arkansas Children's Hospital, Little Rock, AR;

[d]East Carolina University, Greenville, NC;

[e]The Emmes Corporation, Rockville, MD;

[f]See online supplement for full list of Pediatric Trials Network members

Abstract

Background & Aims—Pharmacokinetic data for proton pump inhibitors (PPIs), acid-suppression drugs commonly prescribed to children, are lacking for obese children who are at greatest risk for acid-related disease. In a recent multi-center investigation, we demonstrated decreased, total body weight adjusted, apparent clearance (CL/F) of the PPI pantoprazole for obese children compared with non-obese peers. Subsequently, we developed a population-based pharmacokinetic (PopPK) model to characterize pantoprazole disposition and evaluated appropriate pantoprazole dosing strategies for obese pediatric patients, using simulation.

Methods—Pharmacokinetic data from the only prospective study of PPIs in obese children (6–17 years; n=40) included 273 pantoprazole and 256 pantoprazole-sulfone plasma concentrations, after single oral-dose administration, and were used for pantoprazole model development and covariate analysis (NONMEM®). Model evaluation was performed via bootstrapping and predictive checks, and the final model was applied to simulate systemic pantoprazole exposures for common dosing scenarios.

Results—A 2-compartment PopPK model, which included *CYP2C19* genotype and total body weight, provided the best fit. Resultant, typical, weight-normalized pantoprazole parameter

estimates were different than previously reported for children or adults, with significantly reduced pantoprazole CL/F for obese children. Of the dosing scenarios evaluated, the weight-tiered approach, approved by the US Food and Drug Administration (FDA), achieved pantoprazole exposures (area under the curve [$AUC_{0-\infty}$]) within ranges previously reported as therapeutic, without over- or under-prediction for obese children.

Conclusions—Our data argue against empiric dose escalation of PPIs for obese children and support current FDA-approved pediatric weight-tiered dosing for pantoprazole; however, 3-to-5-fold inter-individual variability in pantoprazole $AUC_{0-\infty}$ remained using this dosing approach.

INTRODUCTION

Proton pump inhibitors (PPIs) are potent acid-suppression drugs that are commonly prescribed to children [1]. Obese children (defined by body mass index [BMI] 95th percentile for age) [2] are 6 times more likely than non-obese children to suffer from gastroesophageal reflux disease (GERD) [3], a condition for which PPIs have become the mainstay of therapy [4]. Currently, dosing recommendations for PPIs are lacking for obese children.

Obesity-related changes in physiology—such as changes in tissue composition and proportion of lean to total body mass [5], increased blood volume and cardiac output [6], decreased kidney and liver function [7], and altered regional blood flow [8], protein binding, and drug metabolism [9]—can affect drug pharmacokinetics (PK) [5–8,10,11]. In a recently completed, multi-center investigation of PPI disposition in obese children, we demonstrated decreased clearance and increased systemic exposure for the PPI pantoprazole in obese children and adolescents compared with historical non-obese pediatric peers [9], highlighting an increased risk for systemic PPI overexposure for obese pediatric patients if total body weight (TBW) dosing is employed, as is common in pediatric practice. Emerging evidence suggests that systemic overexposure to PPIs, specifically area under the concentration time curve (AUC) and peak plasma concentration (C_{max}), may be associated with PPI-related adverse events, such as osteopenic fractures, particularly with prolonged PPI treatment [12]. To help minimize the risk of PPI overexposure for obese children, based on our pharmacokinetic data, we developed a population-based PK model to characterize pantoprazole disposition and evaluated appropriate pantoprazole dosing strategies for obese children.

METHODS

Study Design

PK data from a prospective, multi-center, open-label, single-oral-dose investigation of pantoprazole in 40 obese children (BMI 95th percentile for age, aged 6–17 years) were used for model development. This study (www.clinicaltrials.gov NCT02186652) was conducted in accordance with the ethical standards of the responsible committee on human experimentation (institutional and national) and the current revision of the Declaration of Helsinki. Study participants received pantoprazole (PROTONIX® delayed-release tablets, Wyeth Pharmaceuticals, Inc., Philadelphia, PA), approximately 1.2 mg per lean body weight

(LBW) kilogram calculated via a validated LBW equation [13], rounded to the nearest whole tablet and up to a total maximum dose of 80 mg. All children were genotyped for *CYP2C19*, the primary drug metabolizing pathway for pantoprazole clearance.

Bioanalytical Methods

Pantoprazole and pantoprazole-sulfone concentrations in plasma were quantified by the Pediatric Trials Network's central laboratory (OpAns, LLC, Durham, NC) using a validated high-performance liquid chromatography tandem mass spectrometry (HPLC/MS-MS) assay. The lower limit of quantification for both pantoprazole and pantoprazole-sulfone were 10 ng/mL. During method validation, accuracy and precision of all sample runs were within the FDA bioanalytical assay validation criteria (e.g., ±15%).

Data Analysis

Pantoprazole plasma PK data, following single-time oral administration, were analyzed with a nonlinear mixed effects modeling approach using the software NONMEM® (version 7.2, Icon Solutions, Ellicott City, MD). The first-order conditional estimation method with interaction was used for all model runs. Run management was performed using Pirana (version 2.8.1) [14]. Visual predictive checks and bootstrap methods were performed with Perl-speaks-NONMEM® (version 3.6.2) [15]. Data manipulation and visualization were performed using the software Stata (version 13.1, College Station, TX), R (version 3.0.2, R Foundation for Statistical Computing, Vienna, Austria), and RStudio (version 0.97.551, Rstudio, Boston, MA) with the packages lattice, Xpose, and ggplot2 used for the latter [16].

Based on visual inspection of the PK data, and a review of the primary literature, 1- and 2-compartment PK models were evaluated for both pantoprazole and pantoprazole-sulfone using the ADVAN2 TRANS2 and ADVAN4 TRANS4 subroutines, respectively, in NONMEM®. The population PK analysis was performed using the total dose of pantoprazole, with concentrations of pantoprazole and pantoprazole-sulfone modeled sequentially. The PK parameter estimates from the final model for pantoprazole were fixed in the combined model for pantoprazole and pantoprazole-sulfone (Suppl. Fig. 1). As the fraction of pantoprazole converted to pantoprazole-sulfone has not been reported in the literature, it was fixed to 1 to have an identifiable PK model. Various absorption PK models —including a lag time model, transit compartment model, Erlang absorption model, Weibull absorption model, and sigmoidal Emax absorption model—were evaluated to characterize the delayed absorption of the pantoprazole delayed-release tablet formulation [17–20].

Established methods for addressing bias introduced by below quantification limit (BQL) samples in population PK modeling—including methods M1 (discard all BQL samples), M3 (likelihood-based), M5 (replace BQL samples with the lower limit of quantification [LLOQ]/2), M7 (replace BQL samples with 0), and an all-data approach (include all BQL samples)—were evaluated for BQL samples occurring prior to C_{max} [21,22]. In addition, replacing the BQL data closest and prior to the first measurable PK sample with the LLOQ/2 or 0 were tested. For samples occurring after C_{max}, half the quantification limit was assigned for a single BQL sample, or 0 was assigned for all values in consecutive samples that are BQL. Inter-individual variability (IIV) was assessed for PK model parameters using an

exponential relationship (equation 1). Estimation of a covariance matrix for IIV on clearance (CL) and volume (V) was attempted.

$$P_{ij} = \theta_{Pop,j} * \exp\left(\eta_{ij}\right) \quad (1)$$

where Pij denotes the estimate of parameter j in the ith individual, $\theta_{Pop,j}$ is the population value for parameter j, and ηij denotes the deviation from the average population value for parameter j in the ith individual. The random variable η is assumed to be normally distributed with a mean 0 and variance ω^2. Proportional, additive, and combined (proportional plus additive) residual error models were evaluated (equations 2–4).

$$C_{obs,ij} = C_{pred,ij} * \left(1 + \varepsilon_{prop,ij}\right) \quad (2)$$

$$C_{obs,ij} = C_{pred,ij} + \varepsilon_{add,ij} \quad (3)$$

$$C_{obs,ij} = C_{pred,ij} * \left(1 + \varepsilon_{prop,ij}\right) + \varepsilon_{add,ij} \quad (4)$$

where $C_{obs,ij}$ is the jth observed pantoprazole concentration in the ith individual; $C_{pred,ij}$ is the jth predicted concentration in the ith individual; $\varepsilon_{prop,ij}$ and $\varepsilon_{add,ij}$ are random variables with mean 0 and variance $\sigma_{prop,ij}^2$ and $\sigma_{add,ij}^2$, respectively.

Body size measurements (lean body mass [LBM], fat free mass [FFM], and normal fat mass [NFM]) were calculated using total body weight (TBW) and body height (HT), as shown in equations 9–12 [24–27]. Using a newer pediatric-specific calculation for FFM by Al-Sallami et al [28] did not improve the　in objective function value (OFV; data not shown).

$$LBM = 3.8 * 0.0215 * TBW^{0.6469} * HT^{0.7236} \quad (5)$$

$$\text{For male} \quad FFM = \frac{42.92 * TBW * HT^2}{30.93 * HT^2 + TBW} \quad (6)$$

$$\text{For female} \quad FFM = \frac{37.99 * TBW * HT^2}{35.98 * HT^2 + TBW} \quad (7)$$

$$NFM = FFM + F_{fat} * (TBW - FFM) \quad (8)$$

where F_{fat} is a parameter that accounts for a different contribution of fat mass.

The relationship between body size measurements (TBW, LBM, FFM, and NFM) and PK parameters (CL and V) was explored using a fixed exponent allometric relationship, as shown in equation 13 [26,29,30].

$$P_{ij} = P_j * \left(\frac{W_i}{Wstd}\right)^{PW} \quad (9)$$

where P_{ij} is the estimate of parameter j in the ith individual, W_i is a measure of body size (TBW, LBM, FFM, or NFM) in the ith individual, and P_j is the parameter in an individual with a standard measure of body size (W_{std}). W_{std} is 70 kg, 70 kg, 56 kg, and 52 kg, for TBW, NFM, FFM, and LBM, respectively. The exponent PW is 0.75 for clearance parameters (CL, Q) and 1 for distribution volumes (V_c, V_p).

Covariate Model

The potential effects of clinically significant covariates on PK parameters were evaluated if a relationship was suggested by visual inspection of scatter and box plots (continuous and categorical variables, respectively) of the individual deviations from the population-typical value PK parameters (ETAs) against covariates. The following covariates were explored: age, age group (i.e., adolescent vs. child), BMI, BMI percentile (PBMI), morbid obesity (BMI ≥ 99th percentile), race, sex, LBM, FFM, NFM, waist:hip ratio, $CYP2C19$ genotype (number of functional alleles), and resting energy expenditure (REE). A forward inclusion (p<0.05 and ΔOFV >3.8) and backward elimination (p<0.01 and ΔOFV >6.6) approach was used to evaluate statistical significance of relevant covariates.

With the exception of body size measurements (TBW, LBM, FFM, and NFM) and $CYP2C19$ genotype, continuous covariates were normalized to the population median value as described in equation 14, whereas for categorical covariates such as morbid obesity, a relationship as shown in equation 15 was used.

$$P_{ij} = \theta_{Pop,j} * \left(\frac{cov_i}{cov_m}\right)^{\theta_{cov}} \quad (10)$$

$$P_{ij} = \theta_{Pop,j} * \theta_{cov}^{MORBID\ OBESITY} \quad (11)$$

where cov_i denotes the individual covariate value; cov_m is the population median covariate value; θ_{cov} is a parameter that represents the covariate effect; and *MORBID OBESITY* is a categorical variable that takes on a value of unity when morbidly obese and 0 when non-morbidly obese.

Effect of *CYP2C19* genotype (number of functional alleles) on clearance was evaluated as a continuous variable using equations 16–18.

$$CL_i = \left(\theta_{CL0} + \theta_{2C19} * (n_i)^{0.5}\right) * \left(\frac{TBW_i}{70\ kg}\right)^{0.75} \quad (12)$$

$$CL_i = \left(\theta_{CL0} + \theta_{2C19}^{ni}\right) * \left(\frac{TBW_i}{70\ kg}\right)^{0.75} \quad (13)$$

$$CL_i = \left(\theta_{CL0} + \theta_{2C19} * n_i\right) * \left(\frac{TBW_i}{70\ kg}\right)^{0.75} \quad (14)$$

In equations 16–18, TBW_i denotes the weight of an individual participant; θ_{CL0} is the population estimate for clearance in participants with homozygous loss-of-functional alleles for *CYP2C19*; θ_{2C19} is a parameter that represents the influence of the number of functional alleles on clearance; n_i is the *CYP2C19* number of functional alleles; and CL_i is the estimate of CL of an individual participant.

Model Evaluation

During the population PK model-building process, successful minimization, diagnostic plots, plausibility and precision of parameter estimates, objective function, shrinkage values, and visual predictive checks were used to assess model appropriateness.

Parameter precision for the final population PK model was evaluated using non-parametric bootstrapping (1000 replicates) to generate the 95% confidence intervals for parameter estimates. Standardized visual predictive checks were performed for the final models by generating 1000 Monte Carlo simulation replicates per time point of pantoprazole exposure. Simulated results were compared at the participant level with those observed in the study by calculating and plotting the percentile of each observed concentration in relation to its 1000 simulated observations derived from the final model [31]. The dosing and covariate values used to generate the simulations in the standardized visual predictive check were the same as those used in the study population. The number of observed concentrations outside the 90% prediction interval for each time point was quantified.

Simulation

The modeling results were applied to simulate systemic exposure to pantoprazole (C_{max} and $AUC_{0-\infty}$) after single-time oral drug administration for obese children and adolescents following 3 different dosing scenarios: 1) FDA-approved TBW-tiered dosing for children aged 5 years (20 mg if 15 kg to <40 kg, and 40 mg if 40 kg); 2) 1 mg/kg TBW dosing with a maximum dose of 80 mg, chosen because it falls in the dosing range commonly employed in clinical practice [32]; and 3) 1.2 mg/kg LBW dosing with a maximum dose of 80 mg, recently suggested to be a more appropriate dosing strategy than TBW-based dosing for obese children [9]. Except the participant with 0 functional CYP2C19 allele, all participants used to develop the population PK model (18 obese children and 19 obese adolescents) were included in the simulation. The age in years (median [range]) was 10 (6–11) for obese children, 15 (12–17) for obese adolescents, and 12 (6–17) for all. The total body weight in kg (median [range]) was 53.9 (32.4–123.4) for obese children, 98.6 (67.2–131.6) for obese adolescents, and 79.2 (32.4–131.6) for all. The predicted C_{max} and $AUC_{0-\infty}$ in obese children and adolescents, with the above dosing regimens, were evaluated and compared to reported values in non-obese historical pediatric controls [33] and non-obese adults [34].

RESULTS

Analysis Population

Forty obese pediatric participants (6–17 years) contributed 273 quantifiable pantoprazole and 256 quantifiable pantoprazole-sulfone plasma concentrations (3.1% BQL) after receiving a median single oral dose of pantoprazole 1.11 mg/kg LBW (range 0.82–1.38 mg/kg LBW). Twenty-one participants (52%) had the *CYP2C19* extensive metabolizer (EM) genotype, with 2 functional *CYP2C19* alleles; 18 (45%) were intermediate metabolizers (IMs), with 1 functional *CYP2C19* allele; and 1 participant (3%) was a poor metabolizer (PM), with no functional *CYP2C19* alleles. Participant demographics are summarized in Table 1.

Population PK Modeling Results

A 2-compartment population PK model for both pantoprazole and pantoprazole-sulfone provided the best fit of the data (Figure 1), while the transit compartment model best characterized the delayed absorption PK profiles of pantoprazole. One subject with an atypical absorption profile and one subject with 90% of samples BQL were excluded from the final model (n=38). The M1 method (discard all BQL samples) was selected for addressing bias introduced by BQL samples, as it provided a reasonable fit without convergence issues. Scaling of apparent clearance (CL/F) and apparent volume of distribution (V/F) parameters by TBW using a fixed exponent allometric relationship (exponent = 0.75 for CL/F and 1 for V/F) resulted in the largest reduction in the OFV (OFV=−61.72) compared with LBM (OFV=−58.72), FFM (OFV=−56.1), and NFM (OFV=−62.36) after adjusting for the number of parameters in the model. Additionally, estimating the exponent of TBW on CL/F parameters did not result in a significant drop in OFV (OFV=−0.25) compared with a fixed exponent allometric relationship.

Visual inspection of covariate-parameter relationships identified a relationship between the number of *CYP2C19* functional alleles and CL/F (Figure 2). After incorporating body size, use of a square-root function to quantify the effect of the number of *CYP2C19* functional alleles on CL/F resulted in the largest drop in OFV (OFV=−24.32) compared with other covariates. Incorporation of an effect of waist:hip ratio on V/F and an effect of age on CL/F using a power function also resulted in a significant drop in the OFV; however, only the effect of *CYP2C19* genotype on CL/F was retained after backward elimination.

Standard goodness-of-fit and residual plots of the final model indicated some under-prediction of concentrations at earlier time points; however, considering the large proportion of BQL samples at earlier time points (32 out of 37 pantoprazole samples at 1 hour and 12 out of 40 pantoprazole-sulfone samples at 1.5 hours), the model showed good predictability (Figure 3).

The estimated values for the population PK parameters, covariate and variability, along with the standard error of these estimates and bootstrap medians and the 95% confidence intervals for these values, are summarized in Table 2. In the final model, ETA shrinkage for CL/F, mean transit time (MTT), apparent clearance for pantoprazole-sulfone (CLm/F), apparent volume of distribution for central compartment for pantoprazolesulfone (Vcm/F), apparent distributional clearance for pantoprazole-sulfone (Qm/F), and apparent volume of distribution for peripheral compartment for pantoprazole-sulfone (Vpm/F) were 2%, 0%, 6%, 6%, 24%, and 14%, respectively, while epsilon shrinkage values were 9% and 24% for pantoprazole and pantoprazolesulfone.

Empirical Bayesian estimates (EBEs) obtained from the final model were stratified by age and *CYP2C19* genotype (Table 3). Excluding the only *CYP2C19* PM, individual subject post-hoc CL/F estimates appeared to be higher in children (n=18; 6–11 years) compared with adolescents (n=19; 12–17 years). Half-life was shorter in children, as would be expected with the higher clearance. CL/F in *CYP2C19* EMs was consistently higher than that in *CYP2C19* IMs.

Model Evaluation

The model for pantoprazole and pantoprazole-sulfone was evaluated using a 500-set bootstrap analysis; 83% of bootstrap datasets converged to >3 significant digits. The medians of bootstrap fixed effects parameter estimates were within 6.4% of population estimates from the original dataset for all parameters. The standardized visual predictive check revealed a reasonable fit between the observed and predicted pantoprazole and pantoprazole-sulfone concentrations. A uniform distribution of calculated observation percentiles over the majority of time after dose was observed for pantoprazole and pantoprazole-sulfone (Figure 4). There was some bias toward under-prediction for samples collected at earlier time points. Overall, the percentage of observed concentrations outside of the 90% prediction interval for pantoprazole and its metabolite pantoprazole-sulfone were 10.5% and 4.4%, respectively. The classic visual predictive check showed that the model adequately described the data; the percentages of observed concentrations outside of the 90% prediction interval for pantoprazole and its metabolite were 10.1% and 4.8%, respectively (Figure 5).

Dosing Scenario Simulation Results

Table 4 summarizes the comparison of pantoprazole PK exposures (C_{max} and $AUC_{0-\infty}$) using the population PK model for obese children and adolescents, following 3 dosing scenarios (i.e., FDA-approved weight-tiered dosing, 1.0 mg/kg TBW dosing, and 1.2 mg/kg LBW dosing), to published values for non-obese peers and adults following FDA-approved dosing regimens. Among the 3 evaluated dosing scenarios for pediatric obese patients, the FDA-approved weight-tiered dosing regimen provided the most comparable C_{max} and $AUC_{0-\infty}$ to non-obese peers and non-obese adults. Both TBW-based dosing and LBW-based dosing for obese patients resulted in higher C_{max} and $AUC_{0-\infty}$ values than the FDA-approved weight-tiered dosing regimen, with 1.0 mg/TBW-based dosing leading to the highest C_{max} and $AUC_{0-\infty}$ for obese pediatric patients. As expected from the 500% reduction in CL/F observed in the only *CYP2C19* PM (Table 3), C_{max} and $AUC_{0-\infty}$ were significantly higher for the PM (data not shown). For *CYP2C19* non-PMs (n=37), all dosing scenarios resulted in an approximately 2-fold IIV in pantoprazole C_{max} and 3-to-5-fold IIV in pantoprazole $AUC_{0-\infty}$ (Table 4).

In the absence of pediatric-specific drug exposure-response data for pantoprazole, we compared the drug exposures ($AUC_{0-\infty}$) achieved in the dosing simulations to pantoprazole exposure-response data available for adults (Figure 6). For the most part, systemic exposures achieved for obese pediatric patients fell within pantoprazole $AUC_{0-\infty}$ ranges associated with therapeutic treatment response (e.g., gastric acidity reduction) in adults receiving 40 mg of oral pantoprazole [34–36]. Although all 3 dosing strategies successfully avoided subtherapeutic pantoprazole $AUC_{0-\infty}$ ranges for obese children and adolescents, only the FDA-approved weight-tiered approach avoided systemic exposures above the therapeutic range for adults (Figure 6).

DISCUSSION

Our study illustrates that the typical TBW-normalized PK parameter estimates for pantoprazole, previously reported in the literature for children 6–16 years of age [33,37], do not apply to obese children and adolescents (Table 2). The typical pantoprazole CL/F for obese children (6–11 years) ranged between 0.06 and 0.2 L/kg/h, and for obese adolescents (12–17 years) between 0.04 and 0.15 L/kg/h (compared with 0.4±0.22 and 0.18±0.08 L/kg/h, respectively, previously reported in a pediatric study of non-obese peers by Ward et al [33]). Similarly, the typical apparent steady-state volume of distribution (V_{ss}/F) from our population PK model for obese children and adolescents (0.11 L/kg) was lower than values reported by Ward et al for children (0.4±0.27 L/kg) or adolescents (0.21±0.06 L/kg) [33]. The absorption rate constant (Ka) estimate in our study, median 7.5 h^{-1} (95% CI 2.7–12.2) (Table 2), was greater than the median 1.3 h^{-1} (95% CI 1.05, 1.92) previously reported in a pediatric population analysis by Knebel et al [38]; however, this may be related to differences in the absorption models used and/or the fasting state of participants in our study but not in the Knebel et al study [37].

Previous studies in children [37,38] and adults [39] identified *CYP2C19* genotype as a significant covariate for pantoprazole PK. In our population analysis, the number of *CYP2C19* functional alleles explained variability in pantoprazole CL/F (Figure 2A).

Compared with *CYP2C19* EMs (2 functional alleles), the median pantoprazole CL/F was estimated to be reduced by 18% for IMs (1 functional allele) and by >500% for PMs (no functional alleles) (Table 3). Ratios of CL/F estimates from our population analysis for IM:EM (0.76) and PM:EM (0.18) were comparable to those previously reported for children [37].

Consistent with previous observations of an age effect for *CYP2C19* [33,37,38], our population PK-derived parameter estimates for *CYP2C19* non-PMs (n=37) demonstrated a shorter half-life ($t_{1/2}$) and higher CL/F for the *CYP2C19* substrate pantoprazole in obese children vs. adolescents (Table 3). However, after incorporating *CYP2C19* genotype, age was not identified as a significant covariate in the final population PK model, likely due to the relatively small sample size (n=18 children and n=19 adolescents) and the substantial variability in CL/F. Sex was not identified as a significant covariate, consistent with previous studies [33, 37, 38]. Thus, the final population PK model included genotype and TBW as covariates.

We previously observed that LBW may be a better dosing predictor than TBW for obese pediatric patients [9]. However, in our population PK analysis, LBW failed to account for pantoprazole PK variability any better than TBW. This observation may be explained by a high correlation between LBW and TBW observed in our study population ($\rho=0.91$). Other anthropometric parameters (e.g., waist:hip ratio, resting energy expenditure) were not identified as significant model covariates.

To fill the gap in dosing recommendations for obese pediatric patients, individual estimates from the final model were used to assess the effect of 3 different dosing strategies on pantoprazole exposures for obese pediatric patients: FDA-approved weight-tiered dosing, LBW-based dosing, and TBW-based dosing.

Pantoprazole exposures (C_{max} and $AUC_{0-\infty}$) in obese children and adolescents following the FDA-approved weight-tiered dosing were most comparable to those achieved in non-obese historical peers and non-obese adults using current FDA-approved dosing; whereas, both LBW- and TBW-based dosing resulted in exposures approximately 2-fold greater than reports in non-obese children and adults (Table 4). Given growing concerns regarding the association between PPI overexposure and adverse events (e.g., osteopenia, factures) [32,12], our population data suggest that current FDA-approved weight-tiered dosing for pantoprazole is appropriate for obese pediatric patients.

In contrast to traditional mg-per-kg dosing practices commonly employed in pediatrics [11], where bigger patients receive higher doses of drug, our data argue against empiric dose escalation of PPIs for obese pediatric patients. In addition, these data contradict findings reported in a study of obese adults by Chen et al, which suggested that obese patients need double the pantoprazole dose of non-obese patients to achieve mucosal healing from acid damage [40]; however, PK data were not provided in the adult study. To our knowledge, pantoprazole PK data are lacking in obese adult individuals, as traditionally, these individuals are excluded from clinical trials. Although it is unknown why obesity-related alterations in pharmacokinetics/pharmacodynamics may differ between children and adults,

such differences have been described for some antimicrobials (e.g., cefazolin) but not others (e.g., tobramycin, gentamycin) [35]. It remains to be seen whether the obesity-related changes in pantoprazole PK observed in our pediatric study are true for other PPIs, or other *CYP2C19* substrates prescribed to children, and how these differences may impact pharmacodynamics in obese children.

In the absence of pediatric pharmacodynamic exposure-response data for pantoprazole, we compared the average exposures achieved using the FDA-approved weight-tiered dosing for obese children (C_{max} 3.69±1.08 mcg/mL, $AUC_{0-\infty}$ 5.9±2.0 mcg*h/mL) and adolescents (C_{max} 2.58±0.61 mcg/mL, $AUC_{0-\infty}$ 4.7±1.9 mcg*h/mL) with data available in adults (C_{max} 2.51±0.67 mcg/mL, $AUC_{0-\infty}$ 4.6±2.0 mcg*h/mL). Exposures achieved in obese pediatric patients fell within ranges previously associated with therapeutic treatment response (e.g., gastric acidity reduction) for adults receiving 40 mg of oral pantoprazole [36,41,34] (Figure 6). However, using this dosing approach still resulted in 3-to-5-fold IIV in $AUC_{0-\infty}$. Thus, even outside of *CYP2C19* phenotype extremes (e.g., PMs), which are rare, commonly encountered genetic variants in *CYP2C19* may be important determinants of PPI pharmacodynamics, both in terms of PPI efficacy and potential adverse events associated with higher systemic exposures to PPIs over time (e.g., osteopenia) [12].

Although our population model is based on a relatively small sample size (n=40), it is the only published model of PPI PK for obese children. Model-derived PK parameters were substantially different from those previously reported for non-obese children [38], who were not included in this study, as the study objective was to describe pantoprazole PK specifically for obese children.

Conclusion

Our findings regarding pantoprazole PK in obese children and adolescents are novel, highly relevant, and clinically important in light of the pediatric obesity epidemic [42]. Clinicians currently prescribe therapies for obese children and adolescents without clear dosing recommendations for up to 1 in 6 patients [2]. In contrast to traditional mg-per-kg dosing practices commonly employed in pediatrics [11], our simulation data argue against empiric dose escalation of PPIs for obese pediatric patients and support the current FDA-approved pantoprazole weight-tiered dosing strategy for obese children and adolescents, without dose escalation.

Supplementary Material

Refer to Web version on PubMed Central for supplementary material.

Acknowledgments

REFERENCES

1. Chai G, Governale L, McMahon AW, Trinidad JP, Staffa J, Murphy D. Trends of outpatient prescription drug utilization in US Children, 2002–2010. 2012;130:23–31.

2. Ogden CL, Carroll MD, Kit BK, Flegal KM. Prevalence of childhood and adult obesity in the United States, 2011–2012. JAMA. 2014;311:806–14. [PubMed: 24570244]

3. Koebnick C, Getahun D, Smith N, Porter AH, Der-Sarkissian JK, Jacobsen SJ. Extreme childhood obesity is associated with increased risk for gastroesophageal reflux disease in a large population-based study. Int J Pediatr Obes. 2011;6:e267–63.

4. Gibbons TE, Gold BD. The use of proton pump inhibitors in children: a comprehensive review. Paediatr Drugs. 2003;5:25–40.

5. Cheymol G Effects of obesity on pharmacokinetics: implications for drug therapy. Clin Pharmacokinet. 2000;39:215–31. [PubMed: 11020136]

6. Brill MJE, Diepstraten J, van Rongen A, van Kralingen S, van den Anker JN, Knibbe CA. Impact of obesity on drug meatabolism and elimination in adults and children. Clin Pharmacokinet. 2012;51:277–304. [PubMed: 22448619]

7. Harskamp-van Ginkel MW, Hill KD, Becker KC, Testoni D, Cohen-Wolkowiez M, Gonzalez D, et al. Drug dosing and pharmacokinetics in children with obesity: a systematic review. JAMA Pediatr. 2015;169:678–85. [PubMed: 25961828]

8. Knibbe CA, Brill MJ, van Rongen A, Diepstraten J, van der Graaf PH, Danhof M. Drug disposition in obesity: toward evidence-based dosing. Annu Rev Pharmacol Toxicol. 2015;55:149–67. [PubMed: 25340929]

9. Shakhnovich V, Smith PB, Guptill JT, James LP, Collier DN, Wu H, et al. Obese children require lower doses of pantoprazole than nonobese peers to achieve equal systemic drug exposures. J Pediatr. 2018;193:102–8.e1. [PubMed: 29389444]

10. Rowe S, Siegel D, Benjamin DK, Jr. Gaps in drug dosing for obese children: a systematic review of commonly prescribed emergency care medications. Clin Ther 2015;37:1924–32. [PubMed: 26323523]

11. Kendrick JG, Carr RR, Ensom MH. Pediatric obesity: pharmacokinetics and implications for drug dosing. Clin Ther. 2015;37:1897–923. [PubMed: 26361823]

12. Dubcenco E, Beers-Block PM, Kim L, Schotland P, Levine JG, McCloskey CA, et al. A proton pump inhibitor in the reformulation setting: bioequivalence and potential implications for long-term safety. Clin Transl Sci. 2017;10:387–94. [PubMed: 28618191]

13. Janmahasatian S, Duffull SB, Ash S, Ward LC, Byrne NM, Green B. Quantification of lean bodyweight. Clin Pharmacokinet. 2005;44:1051–65. [PubMed: 16176118]

14. Keizer RJ, van Benten M, Beijnen JH, Schellens JH, Huitema AD. Piraña and PCluster: a modeling environment and cluster infrastructure for NONMEM. Comput Methods Programs Biomed. 2011;101:72–9. [PubMed: 20627442]

15. Lindbom L, Ribbing J, Jonsson EN. Perl-speaks-NONMEM (PsN)--a Perl module for NONMEM related programming. Comput Methods Programs Biomed. 2004;75:85–94. [PubMed: 15212851]

16. Jonsson EN, Karlsson MO. Xpose--an S-PLUS based population pharmacokinetic/pharmacodynamic model building aid for NONMEM. Comput Methods Programs Biomed. 1999;58:51–64. [PubMed: 10195646]

17. Savic RM, Jonker DM, Kerbusch T, Karlsson MO. Implementation of a transit compartment model for describing drug absorption in pharmacokinetic studies. J Pharmacokinet Pharmacodyn. 2007;34:711–26. [PubMed: 17653836]

18. Rousseau A, Léger F, Le Meur Y, Saint-Marcoux F, Paintaud G, Buchler M, et al. Population pharmacokinetic modeling of oral cyclosporin using NONMEM: comparison of absorption pharmacokinetic models and design of a Bayesian estimator. Ther Drug Monit. 2004;26:23–30. [PubMed: 14749545]

19. Desai A Schmitt-Hoffmann AH, Mujais S, Townsend R. Population pharmacokinetics of isavuconazole in subjects with mild or moderate hepatic impairment. Antimicrob Agents Chemother. 2016;60:3025–31. [PubMed: 26953193]

20. Van Wart SA, Shoaf SE, Mallikaarjun S, Mager DE. Population-based meta-analysis of hydrochlorothiazide pharmacokinetics. Biopharm Drug Dispos. 2013;34:527–39. [PubMed: 24123104]

21. Keizer RJ, Jansen RS, Rosing H, Thijssen B, Beijnen JH, Schellens JH, et al. Incorporation of concentration data below the limit of quantification in population pharmacokinetic analyses. Pharmacol Res Perspect. 2015;3:e00131. [PubMed: 26038706]

22. Beal SL. Ways to fit a PK model with some data below the quantification limit. J Pharmacokinet Pharmacodyn. 2001;28:481–504. [PubMed: 11768292]

23. Holford N, Heo YA, Anderson B. A pharmacokinetic standard for babies and adults. J Pharm Sci. 2013;102:2941–52. [PubMed: 23650116]

24. Hallynck TH, Soep HH, Thomis JA, Boelaert J, Daneels R, Dettli L. Should clearance be normalised to body surface or to lean body mass? Br J Clin Pharmacol. 1981;11:523–6. [PubMed: 7272167]

25. Peters AM, Snelling HL, Glass DM, Bird NJ. Estimation of lean body mass in children. Br J Anaesth. 2011;106:719–23. [PubMed: 21498495]

26. Allegaert K, Olkkola KT, Owens KH, Van de Velde M, de Maat MM, Anderson BJ. Covariates of intravenous paracetamol pharmacokinetics in adults. BMC Anesthesiol. 2014;14:77. [PubMed: 25342929]

27. Anderson BJ, Holford NH. Mechanistic basis of using body size and maturation to predict clearance in humans. Drug Metab Pharmacokinet. 2009;24:25–36. [PubMed: 19252334]

28. Al-Sallami HS, Goulding A, Grant A Taylor R, Holford N, Duffull SB. Prediction of fat-free mass in children. Clin Pharmacokinet. 2015;54:1169–78. [PubMed: 25940825]

29. Habtemariam B, Sallas W, Sunkara G, Kern S, Jarugula V, Pillai G. Population pharmacokinetics of valsartan in pediatrics. Drug Metab Pharmacokinet. 2009;24:145–52. [PubMed: 19430170]

30. Cortinez LI, Anderson BJ, Holford NH, Puga V, de la Fuente N, Auad H, et al., Dexmedetomidine pharmacokinetics in the obese. Eur J Clin Pharmacol. 2015;71:1501–8. [PubMed: 26407689]

31. Wang DD, Zhang S. Standardized visual predictive check versus visual predictive check for model evaluation. J Clin Pharmacol. 2012;52:39–54. [PubMed: 21257797]

32. Cohen S, Bueno de Mesquita M, Mimouni FB. Adverse effects reported in the use of gastroesophageal reflux disease treatments in children: a 10 years literature review. Br J Clin Pharmacol. 2015;80:200–8. [PubMed: 25752807]

33. Ward RM, Kearns GL, Tammara B, Bishop P, O'Gorman MA, James LP, et al. A multicenter, randomized, open-label, pharmacokinetics and safety study of pantoprazole tablets in children and adolescents aged 6 through 16 years with gastroesophageal reflux disease. J Clin Pharmacol. 2011;51:876–87. [PubMed: 20852004]

34. PROTONIX® (pantoprazole sodium) delayed-release tablets and PROTONIX® (pantoprazole sodium) for delayed-release oral suspension [U.S. package insert]. Collegeville, Pa: Wyeth; 2009.

35. Sampson MR, Cohen-Wolkowiez M, Benjamin D, Jr, Capparelli E, Watt K. Pharmacokinetics of antimicrobials in obese children. GaBi J. 2013;2:76–81. [PubMed: 25009734]

36. Clinical Pharmacology and Biopharmaceutics Review(s). Available at: https://www.accessdata.fda.gov/drugsatfda_docs/nda/2000/20987_Protonix_biopharmr_P2.pdf. Accessed September 21, 2017.

37. Kearns GL, Blumer J, Schexnayder S, James LP, Adcock KG, Reed MD, et al. Single-dose pharmacokinetics of oral and intravenous pantoprazole in children and adolescents. J Clin Pharmacol. 2008;48:1356–65. [PubMed: 18664620]

38. Knebel W, Tammara B, Udata C, Comer G, Gastonguay MR, Meng X. Population pharmacokinetic modeling of pantoprazole in pediatric patients from birth to 16 years. J Clin Pharmacol. 2011;51:333–45. [PubMed: 20484619]

39. Tanaka M, Ohkubo T, Otani K, Suzuki A, Kaneko S, Sugawara K, et al. Metabolic disposition of pantoprazole, a proton pump inhibitor, in relation to S-mephenytoin 4'-hydroxylation phenotype and genotype. Clin Pharmacol Ther. 1997;62:619–28. [PubMed: 9433390]

40. Chen WY, Chang WL, Tsai YC, Cheng HC, Lu CC, Sheu BS. Double-dosed pantoprazole accelerates the sustained symptomatic response in overweight and obese patients with reflux

esophagitis in Los Angeles grades A and B. Am J Gastroenterol. 2010;105:1046–52. [PubMed: 19904250]

41. Available at: https://www.accessdata.fda.gov/drugsatfda_docs/…/20988_Protonix_biopharmr.pdf Accessed September 21, 2017.

42. World Health Organization. Global strategy on diet, physical activity and health: childhood overweight and obesity. Available at: http://www.who.int/dietphysicalactivity/childhood. Accessed August 16, 2017.

Key Points

Proton pump inhibitors (PPIs) are commonly prescribed medications for children, without clear dosing recommendations for obese children and despite growing evidence for dose-dependent adverse events. Drug clearance for the PPI pantoprazole is reduced in obese children compared to non-obese children or adults. Counterintuitive to traditional pediatric weight-based dosing, our data demonstrate that obese children do not require higher pantoprazole doses than non-obese children, to achieve comparable drug levels.
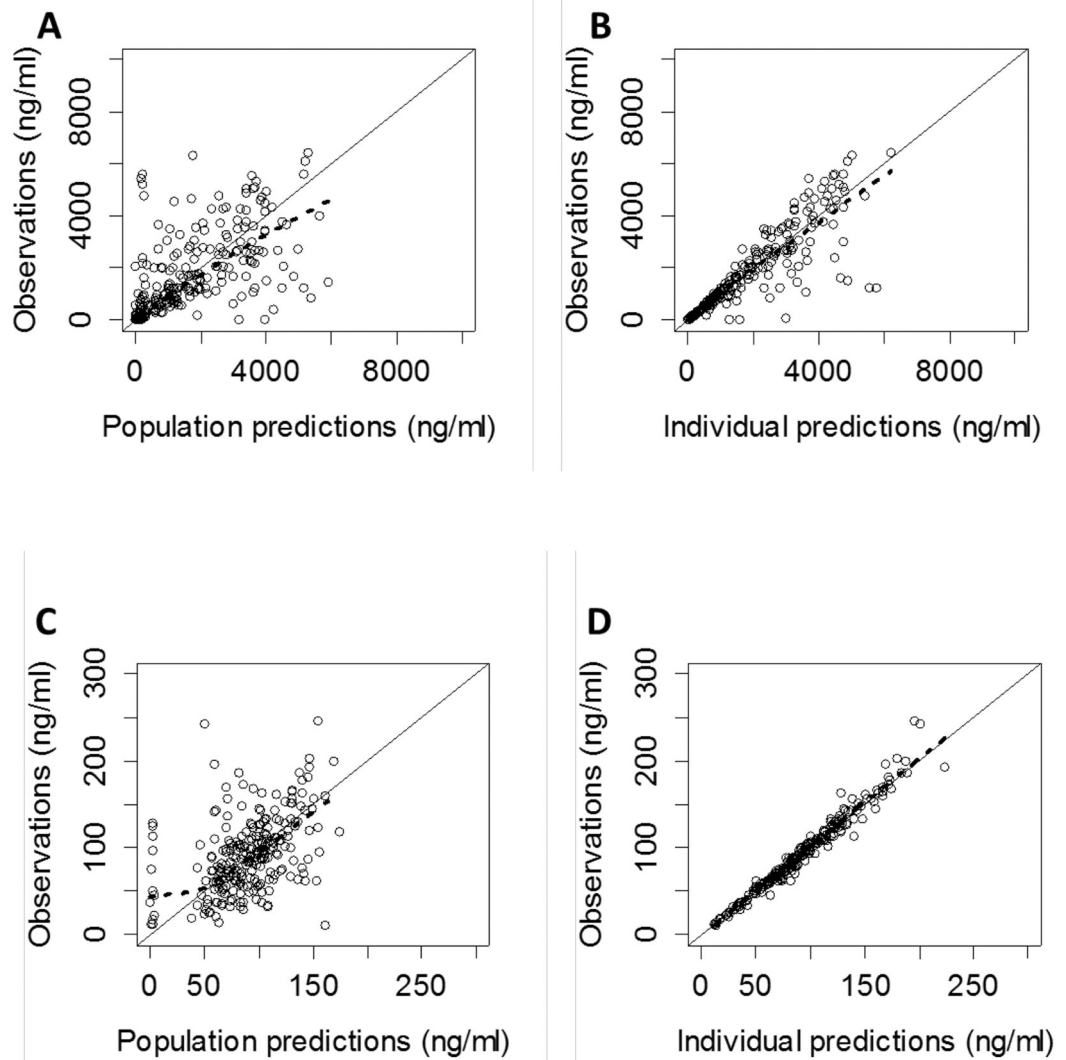
Figure 1.
Observed vs. population (A & C) and individual (B & D) predictions for plasma concentrations of pantoprazole (top) and its minor, CYP3A4-mediated inactive metabolite, pantoprazole-sulfone (bottom), in the final model.
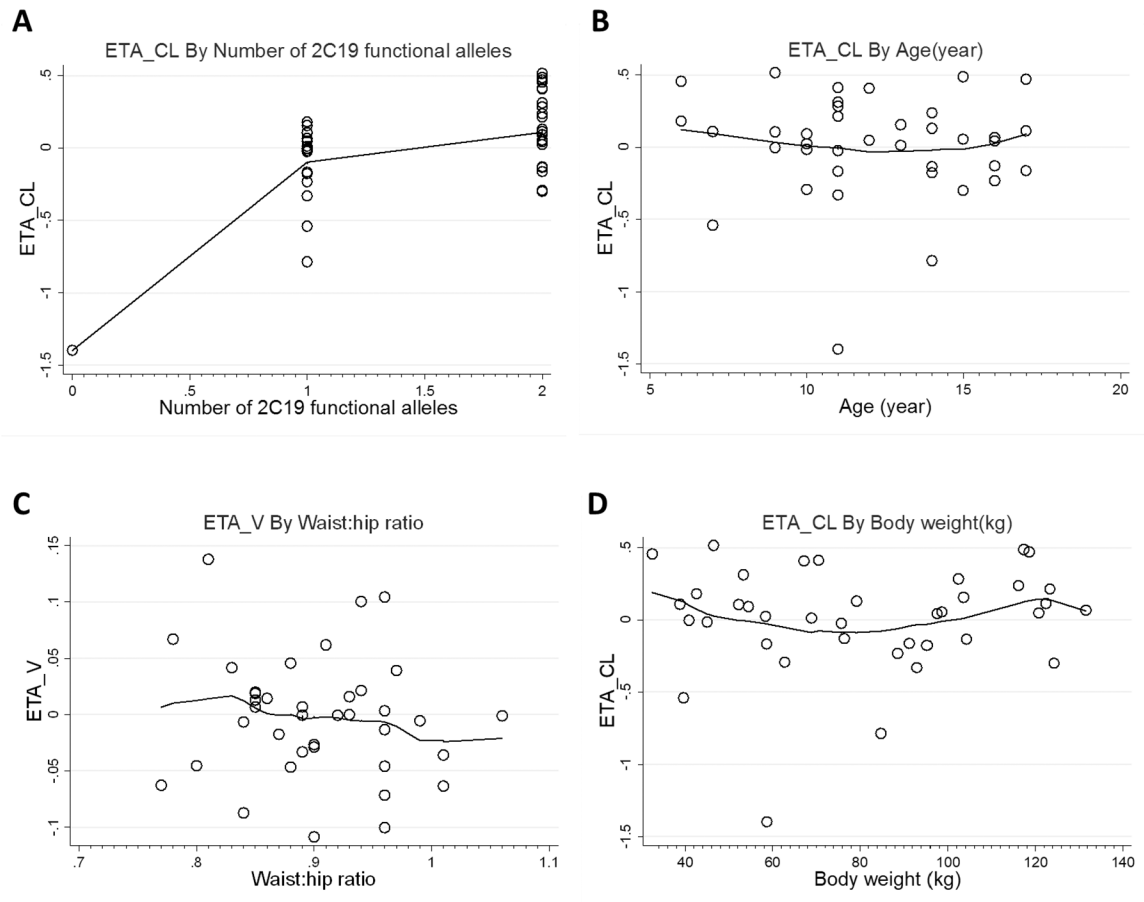
Figure 2.
The difference between an individual's parameter and the population value (ETA) for clearance (ETA_CL) vs. *CYP2C19* genotype (A), clearance (ETA_CL) vs. age (B), volume of distribution (ETA_V) vs. waist:hip ratio (C) and clearance (ETA_CL) vs. total body weight (D) in the base pantoprazole pharmacokinetic model.
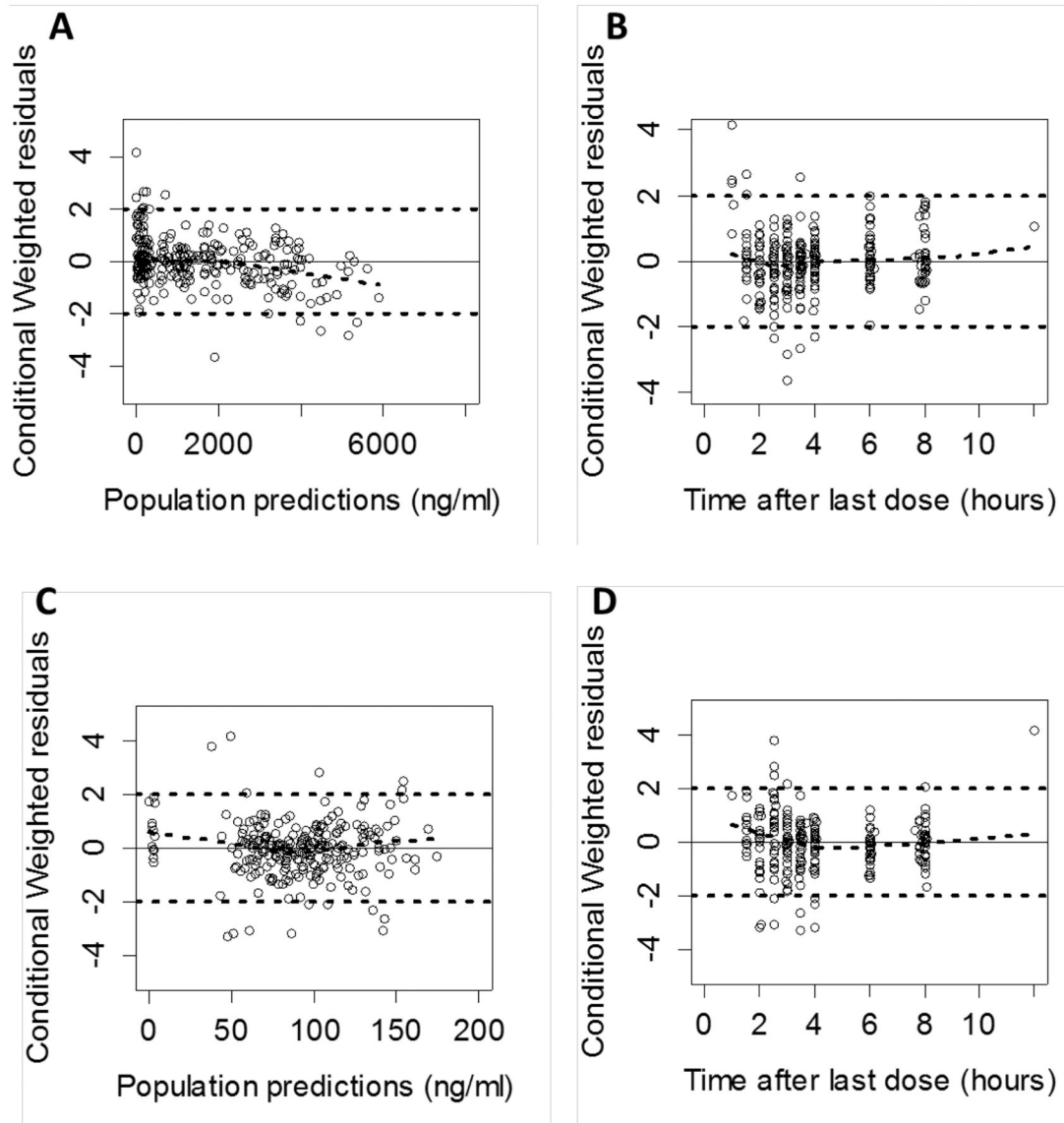
Figure 3.
Conditional weighted residuals vs. population predictions (A & C) and time after oral dose (B & D) for pantoprazole (top) and pantoprazole-sulfone (bottom) in the final model.
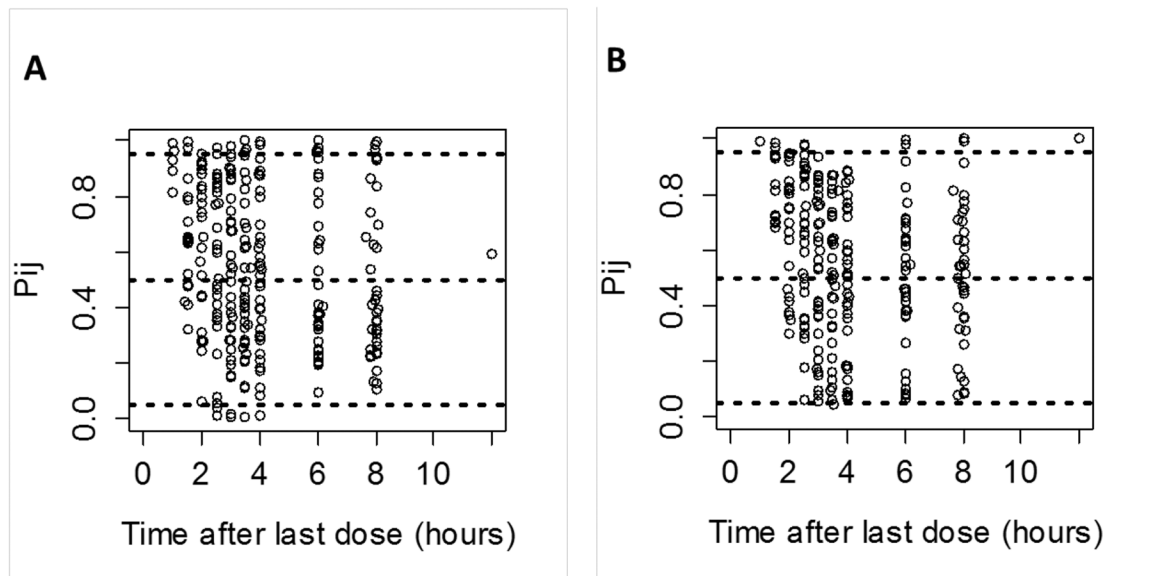
Figure 4.
Standardized visual predictive check of pantoprazole (A) and pantoprazole-sulfone (B) observation percentiles vs. time after single oral dose. Open circles represent calculated percentiles. Dashed lines represent the 5th, 50th, and 95th percentiles (bottom, middle, and top, respectively) of model-predicted data.

Figure 5.
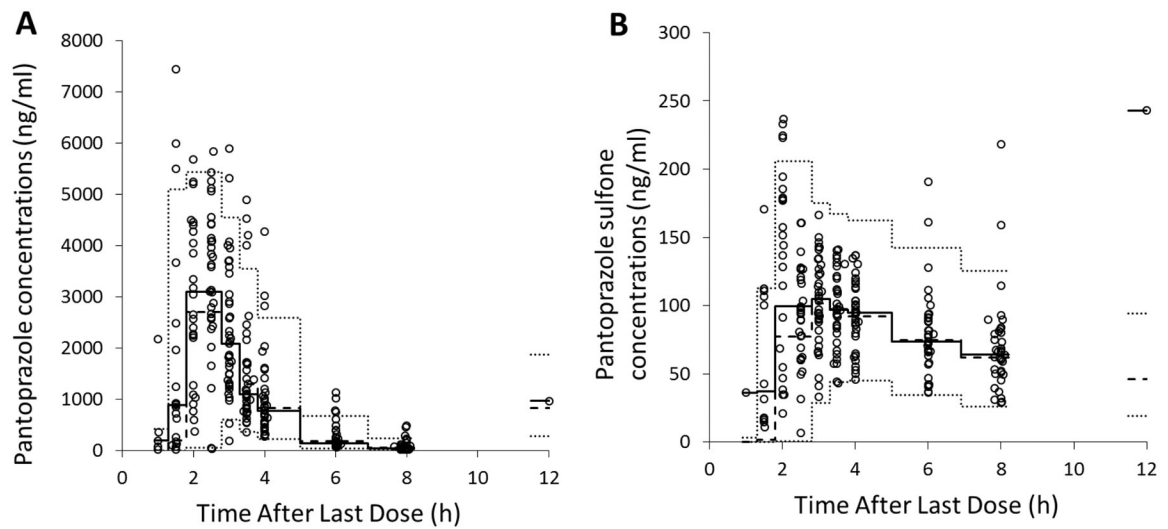Visual predictive check of pantoprazole (A) and pantoprazole-sulfone (B) in the final population pharmacokinetic model. Top and bottom dashed lines are the 97.5th and 2.5th percentiles for the simulated data; middle dashed line is the median for the simulated data; middle solid line is the median for the observed data. Open circles contain the observed data collected across all subjects.
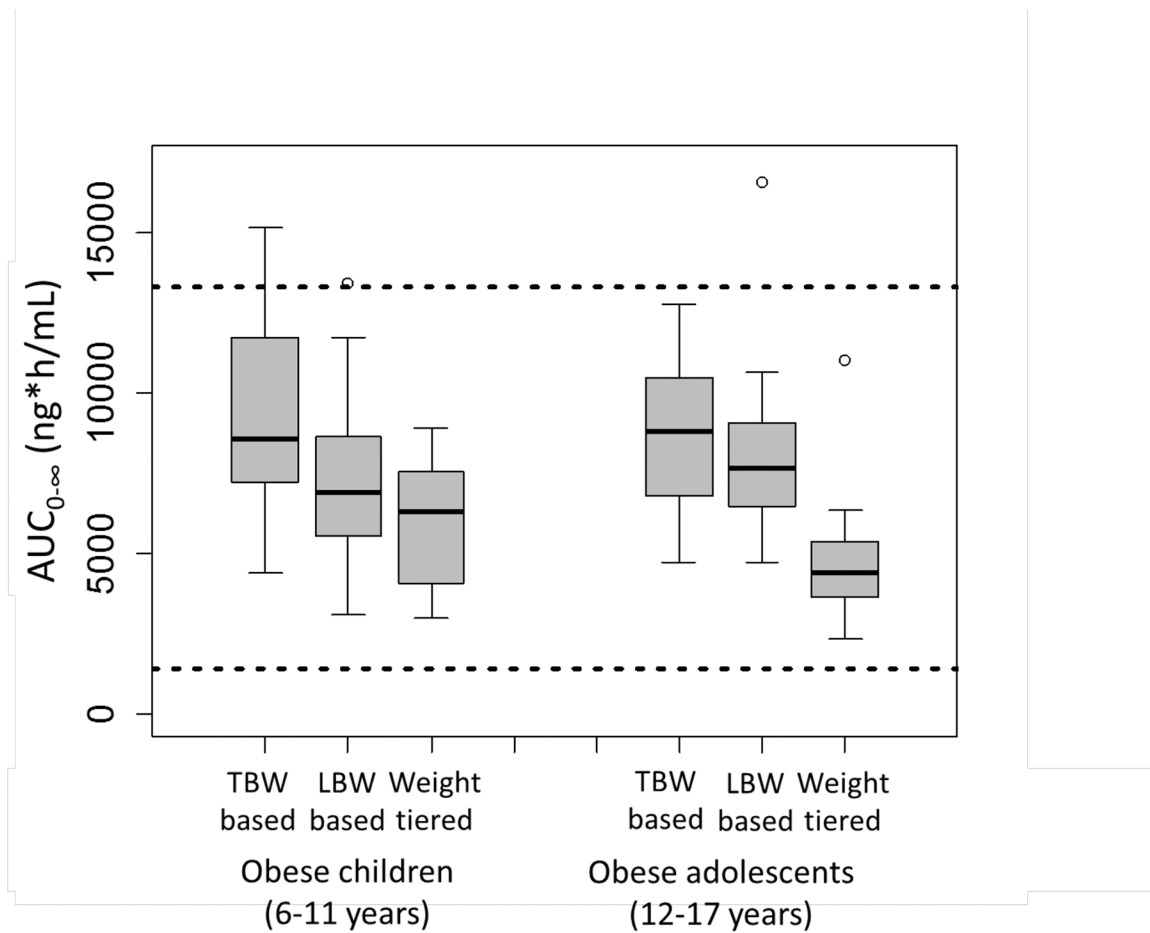
Figure 6.

Pantoprazole $AUC_{0-\infty}$ predicted using population pharmacokinetic model in obese children (n=18) and adolescents (n=19) following total body weight (TBW)-based dosing (1 mg/kg TBW), lean body weight (LBW)-based dosing (1.2 mg/kg LBW), and FDA-approved weight-tiered pantoprazole dosing (20 mg for weight 15–39 kg and 40 mg for weight 40 kg), compared to published reported values in adults. Dashed lines represent the range of data from a one-time oral administration of 40 mg pantoprazole to adult extensive metabolizers. The total body weight (median [range]) was 53.9 (32.4–123.4) for obese children, 98.6 (67.2–131.6) for obese adolescents, and 79.2 (32.4–131.6) for all.

Table 1.

Demographic characteristics of the 40 obese pediatric participants in the pharmacokinetic analysis and model development.

Variable	Median (range) or N (%)		
	Age 6–11 yrs	Age 12–17 yrs	All
N	19	21	40
Age (years)	10 (6–11)	14 (12–17)	12 (6–17)
Total body weight (kg)	54.5 (32.4–123.4)	97.5 (67.2–131.6)	77.6 (32.4–131.6)
Lean body weight (kg)	35.0 (21.0–60.2)	55.5 (43.1–81.4)	48.7 (21.0–81.4)
Body mass index (kg/m^2)	25.3 (22.1–42.0)	36.5 (26.8–41.5)	29.9 (22.1–42.0)
Waist:hip ratio	0.90 (0.81–1.01)	0.88 (0.77–1.09)	0.90 (0.77–1.09)
Resting energy expenditure (kcal)	1580 (750–2090)	2110 (1420–2910)	1810 (750–2910)
Female	12 (63)	10 (48)	22 (55)
Race			
White	8 (42)	12 (57)	20 (50)
Black or African American	7 (37)	5 (24)	12 (30)
Asian	1 (5)	0 (0)	1 (2.5)
Other	3 (16)	4 (19)	7 (17.5)
Obesity status			
Obese	15 (79)	13 (62)	28 (70)
Morbidly obese	4 (21)	8 (38)	12 (30)
CYP2C19 genotype			
Poor metabolizer	1 (5)	0 (0)	1 (3)
Intermediate metabolizer	9 (47)	9 (43)	18 (45)
Extensive metabolizer	9 (47)	12 (57)	21 (52)

Data are median (range) for continuous variables or N (%) for categorical variables.

Table 2.

Parameter estimates for the final population pharmacokinetic model for pantoprazole and pantoprazole-sulfone.

Parameter	Estimate	RSE (%)	2.5th %ile	Bootstrap* median	97.5th %ile
Structural model					
$Ka^{\#}$ (1/h)	7.49	32	4.66	7.97	17.4
$CL/F=\theta_{CL0}+\theta_{2c19}*n_1^{0.5}$ (L/h, 70 kg)					
$\theta_{CL0}^{\#}$	1.45	12	1.15	1.47	1.75
$\theta_{2C19CL}^{\#}$	4.64	6	4.09	4.65	5.16
$Vc/F^{\#}$ (L, 70 kg)	6.06	10	5.23	5.94	6.61
$Q/F^{\#}$ (L/h, 70 kg)	1.86	29	1.20	1.97	3.09
$Vp/F^{\#}$ (L, 70 kg)	1.61	20	1.17	1.68	2.25
$N^{\#}$	63.2	24	42.2	60.2	82.9
$MTT^{\#}$ (h)	1.82	5	1.65	1.82	2.01
Fm	1 FIX	NA	NA	NA	NA
CLm/F (L/h, 70 kg)	44.5	12	38.1	44.1	49.5
Vcm/F (L, 70 kg)	32.7	32	18.0	33.1	56.0
Qm/F (L/h, 70 kg)	274	8	237	271	328
Vpm/F (L, 70 kg)	310	7	275	309	358
Inter-individual variability (% CV)					
CL/F	26.9	21	21.9	26.4	32.1
MTT	28.5	21	22.3	28.3	34.7
CLm/F	60.7	59	50.5	59.8	69.8
Vcm/F	140.7	49	95.6	134	181
Qm/F	23.6	47	10.9	22.8	37.3
Vpm/F	34.4	37	23.2	33.8	48.4
Residual error					
Proportional error, pantoprazole (%)	26.7	22	21.9	26.8	30.4
Proportional error, pantoprazole-sulfone (%)	9.2	28	7.3	9.1	10.9

*1000 bootstrap runs were performed for pantoprazole pharmacokinetic parameters (Ka, θ_{CL0}, θ_{2C19}, Vc/F, Q/F, Vp/F, N, MTT); 500 bootstrap runs were performed for pantoprazole-sulfone pharmacokinetic parameters (CLm/F, Vcm/F, Qm/F, Vpm/F), inter-individual variability, and residual error parameters.

#PK parameters, RSE and bootstrap results of pantoprazole were fixed to values of the final PK model for pantoprazole. CL/F, apparent clearance for pantoprazole; CLm/F, apparent clearance for pantoprazole-sulfone; CV, coefficient of variation; Fm, bioavailability for pantoprazole-sulfone; Ka, absorption rate constant; MTT, mean transit time; N, number of transit compartments; NA, not available; Q/F, apparent distributional clearance for pantoprazole; Qm/F, apparent distribution clearance for pantoprazole-sulfone; RSE, relative standard error; Vc/F, apparent volume for central compartment for pantoprazole; Vcm/F, apparent volume for central compartment for pantoprazole-sulfone; Vp/F, apparent volume for peripheral compartment for pantoprazole; Vpm/F, apparent volume for peripheral compartment for pantoprazole-sulfone.

The population mean estimate of CL/F (L/h) for an individual should be calculated as $CL/F = \left(\theta_{CL0} + \theta_{2C19} * \left(n_1\right)^{0.5}\right) * \left(\frac{TBW}{70 \; kg}\right)^{0.75}$, where $\theta_{CL0} = 1.45$; $\theta_{2C19} = 4.64$; n_1 is the *CYP2C19* number of functional alleles for the individual; *TBW* is the weight of the individual.

Table 3.

Individual empiric Bayesian post-hoc parameter estimates for pantoprazole in children, excluding the *CYP2C19* poor metabolizer (PM).

Variable	N	CL/F (L/kg TBW/h)	CL/F (L/h)	CL/F (L/h for 70kg TBW)	V_{ss}/F[b] (L/kg TBW)	Half-life (h)
Age						
6–11 years	18	0.11 (0.06–0.20)	6.13 (2.64–13.19)	7.50 (4.04–12.19)	0.11	0.90 (0.65–1.39)
12–17 years	19	0.09 (0.04–0.15)	9.07 (3.65–16.71)	7.01 (3.16–11.30)	0.11	1.09 (0.81–1.94)
2C19 genotype						
Poor metabolizers	1	0.02	1.29	1.47	0.11	3.60
Intermediate metabolizer	16	0.09 (0.04–0.13)	6.00 (2.64–11.62)	6.73 (3.16–7.97)	0.11	1.10 (0.82–1.94)
Extensive metabolizer	21	0.11 (0.06–0.20)	8.97 (4.66–16.71)	7.98 (5.03–12.19)	0.11	0.95 (0.65–1.45)

Data are presented as median (range). V_{ss}/F was calculated as a sum of V_c/F and V_p/F. All participants had the same TBW normalized V_{ss}/F as no inter-individual variability was estimated on V_c and V_p in the final model.

CL/F, apparent clearance; TBW, total body weight; V_{ss}/F, steady-state volume of distribution.

Author Manuscript

Author Manuscript

Author Manuscript

Author Manuscript

Table 4.

C_{max} and $AUC_{0-\infty}$ predicted using population pharmacokinetic model in *CYP2C19* non-PM obese children and adolescents, following the FDA-approved weight-tiered dosing, total body weight-based dosing, and lean body weight-based dosing, and published reported values in non-obese peers and adults.

| | Obese | | | | | | Non-obese | | Adults [34] |
| | Children (age 6–11 yrs) n=18 | | | Adolescents (age 12–17 yrs) n=19 | | | Children (age 6–11 yrs) n=12 [34] | Adolescents (age 12–16 yrs) n=11 [33] | |
Dosing regimen	FDA-approved weight-tiered dosing	LBW-based dosing	TBW-based dosing	FDA-approved weight-tiered dosing	LBW-based dosing	TBW-based dosing	FDA-approved weight-tiered dosing	FDA-approved weight-tiered dosing	FDA-approved dosing
Dose	20 mg (weight 15–39 kg) 40 mg (weight 40 kg)	1.2 mg/kg	1.0 mg/kg	20 mg (weight 15–39 kg) 40 mg (weight 40 kg)	1.2 mg/kg	1.0 mg/kg	40 mg	20 mg (weight 15–39 kg) 40 mg (weight 40 kg)	40 mg
C_{max} (mcg/mL)	3.69 ± 1.08 (2.02–5.45)	4.47 ± 1.12 (2.34–6.59)	5.60 ± 1.08 (3.55–7.46)	2.58 ± 0.61 (1.70–3.41)	4.37 ± 0.76 (3.14–6.35)	4.98 ± 1.09 (3.39–6.75)	1.8	2.2 ± 1.4	2.5
$AUC_{0-\infty}$ (mcg*h/mL)	5.94 ± 1.97 (3.00–8.89)	7.28 ± 2.56 (3.12–13.39)	9.15 ± 2.92 (4.39–15.13)	4.73 ± 1.93 (2.35–11.03)	7.95 ± 2.68 (4.70–16.55)	9.20 ± 3.89 (4.70–22.07)	6.9	4.3 ± 3.1	4.8 (1.4–13.3)

A maximum dose of 80 mg was used in simulation; pharmacokinetic parameters are given as geometric mean or mean ± standard deviation (range), when available. AUC, area under the curve; C_{max}, maximum serum concentration; FDA, US Food and Drug Administration; LBW, lean body weight; PM, CYP2C19 poor metabolizer; TBW, total body weight.